Holocene-Neogene volcanism in northeastern Australia: chronology and eruption history

Benjamin E. Cohen *[1, 2], Darren F. Mark [1], Stewart J. Fallon [3], P. Jon Stephenson [4]

[1] NERC Argon Isotope Facility, Scottish Universities Environmental Research Centre, Rankine Avenue, East Kilbride, G75 0QF, United Kingdom.
[2] School of Geographical and Earth Sciences, University of Glasgow, G12 8QQ, United Kingdom.
[3] Research School of Earth Sciences, Australian National University, Acton ACT 0200, Australia.
[4] Deceased, School of Earth Sciences, James Cook University, Townsville, Queensland 4811, Australia.

* Corresponding author, email: ben.cohen@glasgow.ac.uk

Abstract

Quaternary and late Neogene volcanism is widespread in northeastern Australia, producing at least 397 eruptions covering more than 20,000 km^2, including at least 20 flows over 50 km long. Despite this abundance of young volcanism, before this study numerous eruptions had tentative ages or were undated, and the area requires a comprehensive evaluation of eruption patterns through time. To help address these issues we applied multi-collector ARGUS-V ^{40}Ar/^{39}Ar geochronology to determine the age of four of the younger extensive flows: Undara (160 km long, 189 ± 4/4 ka; 2σ, with full analytical/external uncertainties), Murronga (40 km long, 153 ± 5/5 ka), Toomba (120 km long, 21 ± 3/3 ka), and Kinrara (55 km long, 7 ± 2/2 ka). Verbal traditions of the Gugu Badhun Aboriginal people contain features that may potentially describe the eruption of Kinrara. If the traditions do record this eruption, they would have been passed down for 230 ± 70 generations – a period of time exceeding the earliest written historical records. To further examine north Queensland volcanism through time we compiled a database of 337 ages, including 179 previously unpublished K-Ar and radiocarbon results. The compiled ages demonstrate that volcanic activity has occurred without major time breaks since at least 9 Ma. The greatest frequency of eruptions occurred in the last 2 Ma, with an average recurrence interval of <10-22 ka between eruptions. Activity was at at times likely more frequent than these calculations indicate, as the geochronologic dataset is incomplete, with undated eruptions, and intraplate volcanism is often episodic. The duration, frequency, and youthfulness of activity indicate that north Queensland volcanism should be considered as potentially still active, and there are now two confirmed areas of Holocene volcanism in eastern Australia – one at each end of the continent. More broadly, our data provides another example of ^{40}Ar/^{39}Ar geochronology applied to Holocene and latest Pleistocene mafic eruptions, further demonstrating that this method has the ability to examine eruptions and hazards at the youngest volcanoes on Earth.

Keywords

Undara; Toomba; Kinrara; ^{40}Ar/^{39}Ar; K-Ar; radiocarbon

Highlights

- North Australian volcanism: >397 eruptions, >20,000 km^2, >20 flows >50 km long.
- Eruptions since 9 Ma, eruption frequency <10-22 ka.
- ^{40}Ar/^{39}Ar ARGUS-V ages extend into the Holocene (Kinrara: 7 ± 2 ka, 2σ).
- Kinrara eruption possibly in Aboriginal verbal traditions for 230 ± 70 generations.

1. Introduction

Quaternary and late Neogene volcanism in northern Queensland, Australia is widespread, covering >20,000 km^2, and is noteworthy for an unusual abundance of exceptionally long lava flows, with at least 20 flows that exceed 50 km (Fig. 1, 2) (Stephenson et al., 1998). Many of the eruptions have well-preserved geomorphic features, including cones, craters, lava levees, lava tubes, tumuli, pressure ridges, and fresh exposed lava surfaces (Fig. 2, 3) (Stephenson et al., 1998; Atkinson, 2010). These features indicate young eruption ages to remain uneroded in this low-latitude region with high-intensity rainfall (Fielding and Alexander, 1996; Alexander et al., 2001). Geochronological analyses also indicate youthful volcanism, with the Toomba and Kinrara eruptions yielding K-Ar ages of considerably less than 100 ka (Table 1), and are likely substantially younger, as the K-Ar results are considered maxima (Wyatt and Webb, 1971; Griffin and McDougall, 1975).

A young age for Toomba is also indicated by radiocarbon (^{14}C) dating of material from beneath the flow (Stephenson et al., 1978). Small carbonized stems and finer disseminated carbonized material found in the lava-baked sand and loam at the banks of the Burdekin River yielded acid-treated, uncalibrated conventional radiocarbon dates ranging from 2,390 to 13,100 BP, with six of the nine dates exceeding 10,000 BP (Stephenson et al., 1978). The youngest three ages were interpreted as being contaminated by younger carbon, with the oldest uncalibrated age of 13,100 ± 200 BP considered the most closely related to burial under hot lava (Stephenson et al., 1978). Nevertheless, these radiocarbon analyses are uncalibrated, and must therefore be re-assessed using modern calibration curves (Hogg et al., 2013). The discrepancy between the radiocarbon and K-Ar results for Toomba also needs to be addressed.

To better constrain eruption ages in north Queensland, we undertook incremental-heating $^{40}Ar/^{39}Ar$ geochronologic analyses of four eruptions, targeting the youngest long flows: Undara (160 km long), Murronga (40 km long), Toomba (120 km long), and Kinrara (55 km long) (Fig. 2). We have also compiled a chronologic database for the region, including 179 previously unpublished K-Ar and radiocarbon analyses, calibrated and reassessed the Toomba radiocarbon ages, and used this integrated dataset to examine the temporal history of volcanism in northeastern Australia.

2. Geological background

In this section we briefly outline how the volcanism in north Queensland fits into the broader picture of Cenozoic intraplate volcanism in eastern Australia. We then describe the geology of the four long lava flows analysed by $^{40}Ar/^{39}Ar$.

2.1 North Queensland and Australian intraplate volcanism

The eruptions in north Queensland form part of the 1,600,000 km^2 of intraplate magmatism extending along the east Australian continental margin (Fig. 1) (Johnson, 1989). This activity spans the Cenozoic, with two main geomorphologic and petrologic types of edifice: central volcanoes and lava field volcanoes (Wellman and McDougall, 1974), and a third, volumetrically minor type, the leucitite volcanoes (Wellman and McDougall, 1974; Cohen et al., 2008). The central volcanoes become progressively younger from 34 Ma at Cape Hillsborough in central Queensland to 6 Ma at Macedon in Victoria, indicating passage over a hotspot or hotspots (Wilson, 1963), which represents Earth's longest continental hotspot track (Fig. 1) (Wellman and McDougall, 1974; Knesel et al., 2008; Cohen et al., 2013a; Davies et al., 2015). The leucitites also become younger to the south, at a rate matching the central volcanoes (Cohen et al., 2008). In contrast, the lava field volcanoes, with eruptions along the entire eastern margin of the continent (Fig. 1) and ages spanning from >60

Ma to the Holocene, have a much less systematic time-space distribution, and no age progression (Wellman and McDougall, 1974; Vasconcelos et al., 2008).

The youngest volcanoes on the Australian continent – with eruptions in the Pliocene, Pleistocene, and Holocene – are all lava field eruptions, located in southeastern Australia, southeastern Queensland, and northern Queensland (Fig. 1). The Pliocene-Holocene volcanism in southeastern Australia (the Newer Volcanics) and northern Queensland are both widespread, covering >19,000 and >20,000 km^2, respectively (Stephenson and Griffin, 1976; Stephenson et al., 1998; Boyce, 2013), while Pliocene-Pleistocene lavas in the Bundaberg area of southeastern Queensland cover less than 1,000 km^2 (Fig. 1) (Johnson, 1989).

The cause of the young lava field volcanoes in Queensland is not well known. They are not plume-derived, as there is no age progression (Whitehead et al., 2007; Cohen et al., 2013b), and the plume that was responsible for the central volcanoes is currently located southeast of Victoria, on the southern side of Australia; a distance of over 2000 km away from the north Queensland eruptions (Fig. 1). Edge-driven convection, asthenospheric shear, Paleocene rifting, and the influence of changing intraplate stress fields have all been considered as potential mechanisms for various lava field provinces in Australia (Lister and Etheridge, 1989; Demidjuk et al., 2007; Whitehead et al., 2007; Conrad et al., 2011; Sutherland et al., 2012; Davies and Rawlinson, 2014). However, no single model satisfies all observations, and further investigation is required (Vasconcelos et al., 2008).

2.2 Geology of the long lava flows in north Queensland

The Undara hawaiite is the longest recorded Cenozoic flow in Australia, and one of the longest on the planet – it surpasses Hawaiian or Icelandic flows (Self et al., 1998), is of similar length to the Pampas Onduladas flow in Argentina (Espanon et al., 2014), and is only exceeded by lavas in the Columbia River Flood Basalts (Self et al., 1998). The Undara vent is 1020 m above sea level and is the highest point of the McBride province (Fig. 2). The vent is 425 m wide, has a summit crater 330 meters across and 60 m deep, but the vent only rises 10-40 m above the surrounding plain (Atkinson et al., 1975; Stephenson et al., 1998). Lavas flowed in several directions, with the western branch of Undara exceeding 160 km from the source crater, while a second branch flowed 90 km north, and a third branch spread east; the entire flow covers about 1550 km^2 (Fig. 2). Lava surface features are generally not preserved, but in rare places where surface features remain (i.e., cave floors or where buried) they are generally pāhoehoe, with only rare examples of ‘a‘ā (Self et al., 1998; Stephenson et al., 1998). The Undara flow has spectacular examples of lava tubes, which insulated the lava from heat loss, aiding lava transport (Fig. 3a, b) (Keszthelyi and Self, 1998; Stephenson et al., 1998). The lower portion of the Undara flow is notable for a feature called “The Wall” – a ridge 40 km long, typically 200 m wide, and rising up to 20 m above the surrounding lava level (Fig. 2). “The Wall” has been interpreted as a lava inflation feature, and as a terrestrial analogue to sinuous ridges on Mars and the Moon (Atkinson and Atkinson, 1995; Stephenson et al., 1998; Atkinson, 2010).

The Murronga flow, in the south-central McBride Province, has its source at Mount Tabletop, a group of three high symmetrical pyroclastic cones with summit craters (Griffin and McDougall, 1975; Griffin, 1977). The lava flowed to the southwest, extending up to 40 km from the crater and covering 235 km^2 (Fig. 2). The flow has a very rugged surface, with an intricate system of sharp ridges and depressions indicating several flow fronts and pulses of lava (Griffin and McDougall, 1975; Griffin, 1977).

The Toomba eruption is the southernmost flow investigated in this study, being located in the Nulla province (Fig. 2). The vent area is 4 to 5 km across and 100 m high, forming a low-angled but prominent block-strewn area with several low-angle pyroclastic cones (Wyatt and Webb, 1971; Stephenson et al., 1998). The flow has several caves within 4 km of the vent area (Stephenson et al., 1998), and flows extend 120 km downstream, covering 670 km^2 (Fig. 2). Surface features are well preserved, with widespread pāhoehoe (Fig. 3c, d); ʻaʻā is found locally, but is absent from the most distal 10 km of the flow (Stephenson et al., 1998). The flow has a highly irregular internal topography due to flow inflation and pressure ridges (Whitehead and Stephenson, 1998), and these rugged surface features were noted by European explorers in 1845 (Leichhardt, 1847). The lava chemistry changed during the Toomba eruption, ranging from early hawaiite, through basanite, hawaiite, and lastly highly porphyritic hawaiite (Burch, 1991; Stephenson et al., 1998). There may be more than ten chemically distinguishable units (Burch, 1991), although there is no field evidence for significant time breaks during emplacement (i.e., no greater than on the order of 100 years, Stephenson et al., 1998).

The Kinrara volcano, on the southeastern side of the McBride province, has a well-preserved cone 30 m high comprised of interbedded pyroclastic material and thin (~0.5 m) lava sheets (Griffin and McDougall, 1975; Stanton, 1993; Stephenson et al., 1998) (Fig. 3e). The cone has evidence for strong lava fountaining (Griffin and McDougall, 1975; Stanton, 1993; Stephenson et al., 1998). The central crater is 300-400 m wide, 86 m deep (Fig. 3e), and contains a solidified lava lake as well as terraces representing former lava levels (Stephenson et al., 1998). The flow has a complex system of lava tubes within 6 km of the vent (Stephenson et al., 1998). Basanite lavas extend a total of 55 km from the vent, with the last 20 km down the Burdekin River valley, covering an area of 173 km^2 (Fig. 2). Original surface features of ropy pāhoehoe lava are preserved on the flow (Fig. 3f), whereas ʻaʻā surfaces are present within 20 km of the vent, within late-stage channelized flows (Stephenson et al., 1998). The flow has a rough internal topography, which proved a significant barrier to early European exploration (Leichhardt, 1847) and also later land use; the area retains much of the original vegetation cover, and has largely not been used for cattle grazing (Stanton, 1993). There is no soil developed on the flow, and vegetation is only present in cracks extending to the underlying soil, indicating youthful eruption (Fig. 3f) (Stephenson et al., 1998).

These four flows have particularly low gradients (0.2-0.4 degrees, Stephenson et al., 1998). The extreme flow lengths is likely to have been assisted by topographic control, with the lava flowing down shallow drainage channels, being injected under surface crusts, and developing extensive lava tube systems (Stephenson et al., 1998).

Basement rocks in the region are a mixture of Palaeozoic or Proterozoic metamorphic, igneous, and sedimentary units, or early Cenozoic sediments, although for much of their length the long lava flows were emplaced onto earlier mafic units in the McBride or Nulla provinces (Fig. 2). The units of early Cenozoic and older ages underwent variable, often extensive, degrees of lateritic weathering.

3. Methods

Rock samples were obtained from the Australian National University (ANU) archive collection, from specimens analysed by K-Ar (Wyatt and Webb, 1971; Griffin and McDougall, 1975), which allows direct comparison between the existing K-Ar and new $^{40}Ar/^{39}Ar$ results. These samples were inspected in thin section, and chosen as they are largely free of xenoliths, devitrified glass, or amygdales (Wyatt and Webb, 1971; Griffin and McDougall, 1975), although there are minor patches of olivine altering to iddingsite. The archived samples comprised chips 0.71-2 mm in diameter; in this study the material was crushed and sieved to 355-500 µm using a rotary disk mill, washed in water to remove dust, then treated in acid to dissolve the weathering phases that act as a source for atmospheric argon. Acid and water rinses were carried out in an ultrasonic bath at <50°C, and involved ~90 minutes in 3.5 N HCl, a ~10 minute rinse with Millipore water, ~30 minutes in 5% HNO_3, and several rinses in Millipore water, each of ~10 minute duration, to ensure all acid was removed. After washing, the material was dried in an oven at <50°C and re-sieved to remove material <250 µm, with the fine fraction mostly comprising liberated olivine or pyroxene fragments. Groundmass separates (i.e., the crystalline matrix with alteration and phenocryst phases removed) were prepared via paramagnetic separation using a Frantz Isodynamic separator, followed by LMT heavy liquids and hand-picking under a binocular microscope to ensure only the freshest groundmass material remained.

Groundmass separates were then wrapped in Cu-foil and irradiated for 6.6 minutes (~396 seconds) at the 1 MW Cd-lined facility, TRIGA research reactor, Oregon State University, USA. The samples were co-irradiated with the neutron-fluence monitor Alder Creek sanidine. After a cooling period of approximately two months, samples and neutron fluence monitors were analysed at the Scottish Universities Environmental Research Centre (SUERC), United Kingdom, on a GVI ARGUS-V multi-collector mass spectrometer (Mark et al., 2009) with a measured sensitivity of $7x10^{-14}$ mol/V. For neutron fluence monitors Alder Creek sanidine, three crystals (each ~500 µm diameter) were combined in each aliquot; while for the north Queensland samples, typically 100-116 mg was analysed (Appendix A). A larger sample size of 285 mg was heated for the duplicate analysis of 74-82, in order to improve the analytical precision (by measurement of larger ion beams) for this very young material (Appendix A). Neutron-fluence monitors were loaded into a steel pan with circular wells 4 mm diameter; Queensland samples were loaded into copper pans with 13 x 13 mm square wells (35 x 35 mm for 74-82 duplicate). Care was taken to ensure the samples were presented as a monolayer (Barfod et al., 2014).

Before analysis, the pans containing samples were baked under ultra-high-vacuum at temperatures of <150°C for 3-4 days. All neutron-fluence and Queensland samples were heated using a Photon-Machines CO_2 10.4-10.8 µm laser. Neutron fluence monitors were fused in a single step, using a flat circular laser beam 4 mm wide with a total power of 15 Watts, while the Queensland samples were incrementally heated using a flat circular beam 3 mm wide. To enable equal exposure to the laser beam, the laser traversed under computer control over the sample for eight minutes, with a longer time of 23 minutes for the larger well used for the analysis of 74-82 duplicate. The released gases were cleaned by exposure to three SAES GP50 getters, two operated at ~450°C and one at room temperature. Cleaning time was 5 minutes for neutron fluence monitors, 23 minutes for most Queensland samples, and 33 minutes for the 74-82 duplicate. After cleaning, the gas was inlet to the mass spectrometer, where a fourth getter (NP10) operated at room temperature was located near the ionizing source. Additional details of mass spectrometer specifications and operations are found in Mark et al. (2009).

Full-system background measurements were run before every analysis. Background levels for ^{40}Ar were typically <2.8 x 10^{-15} moles, compared to typically 0.1-1.9 x 10^{-13} moles for samples (Appendix A). Air shots were run frequently to monitor mass discrimination, with at least three air shots between every sample (Appendix A). All data regression was undertaken in MassSpec version 8.131. Mass spectrometer discrimination was calculated per AMU using the power law, the average $^{40}Ar/^{36}Ar$ value from all air pipette analyses ($^{40}Ar/^{36}Ar$ of 296.89 ± 0.99, 1 standard deviation, n = 85), and an atmospheric $^{40}Ar/^{36}Ar$ value of 298.56 ± 0.31 (Lee et al., 2006) which has been independently confirmed by Mark et al. (2011). We have used the Alder Creek sanidine age of 1.1891 ± 0.0008 Ma (1σ uncertainty) (Niespolo et al., in press) and the potassium decay constants reported by Renne et al. (2011). Full details of other decay constants and irradiation parameters are contained in Appendix A. All uncertainties in Appendix A are reported at the 1σ level, while all age uncertainties in the text and figures are reported at the 2σ level. Age uncertainties in the paper are reported as age ± Y/Z, where Y is analytical precision and Z is the full external precision, including uncertainty from the neutron fluence standard and decay constants (e.g., Renne et al., 2013). We note that in this study, adding the uncertainty in the neutron fluence standard and decay constants does not significantly increase the overall uncertainty of the measurements, as the small uncertainty due to the decay constants is negligible relative to the analytical precision for these very young samples.

4. Results

The analytical results are summarized in Table 1, with incremental step-heating diagrams shown in Fig. 4 and 5, and isotope-correlation plots (which define inverse isochrons) in Fig. 6. Multiple samples from the Undara, Toomba, and Kinrara flows were analysed to ensure the results were reproducible.

For all samples analysed, K/Ca values are generally between 0.5 and 1 for low- and medium-temperature steps, before sharply decreasing to <0.1 at high temperatures (Fig. 4, 5). This behaviour is consistent with the late-crystallizing K-rich material degassing first, with more Ca-rich plagioclase and pyroxene being degassed at high temperatures. Whole-rock potassium contents (from the K-Ar analyses) range from 1.34 to 1.76 wt% K (Table 1). Percent radiogenic argon (%^{40}Ar*) values range from a maximum of 47% for Undara to <4% for Kinrara (Fig. 4, 5, Appendix A). GA5769 (Toomba, Fig. 5c) yielded lower percent radiogenic values compared to the other specimens from that flow, with the extra atmospheric argon likely due to minor amounts of altered phases, mesostasis, or devitrified glass in this specimen.

All samples yielded highly concordant ages, forming very well defined plateaus; eight out of the nine samples have plateaus comprising 100% of the ^{39}Ar released (Fig. 4, 5). The only exception was the duplicate analysis of sample 74-82 (Kinrara, Fig. 5f), which has a single discordant step at the highest temperature, although the plateau still comprises 98% of the ^{39}Ar released. The older age obtained for the high-temperature step may represent a small amount of excess argon (e.g., contained in olivine/pyroxene phenocrysts or disaggregated xenoliths) although the low amount of Ar released and occurrence in only one step make this possibility difficult to evaluate. All samples confirm with the plateau definitions of Fleck et al. (1977) and McDougall & Harrison (1999), namely three or more contiguous steps that represent more than 50% of the ^{39}Ar released that overlap within 95% confidence.

The incremental-heating results from each lava flow are very reproducible; all plateau ages for each flow overlap within two-sigma uncertainty (Fig. 4, 5). We have therefore combined the data from each flow for inverse isochron analysis, with the single non-plateau step excluded (Fig. 6). The four samples yield single-population arrays on the inverse isochrons, and initial $^{40}Ar/^{36}Ar$ intercepts within uncertainty of atmosphere (Fig. 6). With the exception of the excluded step from 74-82 duplicate (as discussed above), these characteristics are diagnostic of well-behaved samples that contain little or no appreciable excess or inherited argon, that have remained essentially undisturbed since eruption, and did not experience appreciable nuclear recoil during irradiation (McDougall and Harrison, 1999). Because the samples are well behaved, we have combined all of the analyses from each flow (excluding the single outlier from 74-82 duplicate) and calculated weighted mean ages for each flow (Table 1). As the trapped $^{40}Ar/^{36}Ar$ values are within uncertainty of the present-day atmosphere for all samples, we use the weighted mean results as the best age estimate for each eruption, which are: 189 ± 4/4 ka for Undara, 153 ± 5/5 ka for Murronga, 21 ± 3/3 ka for Toomba, and 7 ± 2/2 ka for Kinrara (Table 1). The young age for Kinrara is significant as it provides another example of $^{40}Ar/^{39}Ar$ geochronology applied to a Holocene mafic eruption (e.g., Wijbrans et al., 2011).

5. Discussion

5.1 Comparison with K-Ar chronology

The use of the same hand samples for $^{40}Ar/^{39}Ar$ and K-Ar enables direct comparison between the techniques. The advantages of using incremental heating procedures to progressively degas samples and separate radiogenic from atmospheric reservoirs are evident with the much higher $^{40}Ar^*$ in many of the $^{40}Ar/^{39}Ar$ steps, as compared to K-Ar where all the Ar must be extracted in one step. This observation is exemplified by the analyses from Undara, where the highest $\%^{40}Ar^*$ value recorded by $^{40}Ar/^{39}Ar$ was 47% (Fig. 4a, b, Appendix A), as compared to 6.4 and 16.9% for K-Ar (Table 1). The higher $\%^{40}Ar^*$ values from the incremental-heating $^{40}Ar/^{39}Ar$ analyses also likely benefit from two other factors. The first is the ability to analyse a much smaller aliquot (~100 mg vs. several grams for K-Ar), which allows for greater manual removal of weathered phases and non potassium-bearing minerals olivine and pyroxene, and improved analytical blanks. The second factor is the acid pre-treatment of the samples to further remove weathering phases such as iddingsite or calcite – mineral phases that can be subtle or microscopic and difficult to fully separate manually, and are thus best removed chemically.

The comparison between the K-Ar and $^{40}Ar/^{39}Ar$ ages is generally good, especially considering the generally low levels of $^{40}Ar^*$ in these samples (Table 1). For Undara, the $^{40}Ar/^{39}Ar$ and K-Ar ages overlap, with the $^{40}Ar/^{39}Ar$ age benefiting from improved precision obtainable from a multi-collector noble gas mass spectrometer and higher $\%^{40}Ar^*$ yields. The $^{40}Ar/^{39}Ar$ age for Murronga (153 ± 5/5 ka) just overlaps with and is intermediate between the two recalculated K-Ar ages (120 ± 40 and 190 ± 30 ka, Table 1). Griffin & McDougall (1975) noted that material from Murronga proved challenging for K-Ar analysis as it contains a significant percentage of mesostasis, the effects of which would be minimised by the sample preparation (e.g., acid pre-treatment) and incremental heating techniques employed for $^{40}Ar/^{39}Ar$ geochronology (Fig. 4c). Nevertheless, the average of the two K-Ar measurements (155 ± 30 ka) from Murronga is similar to the $^{40}Ar/^{39}Ar$ measurement. The results from Undara and Murronga show that $^{40}Ar/^{39}Ar$ and K-Ar can yield concordant results – at least in these two samples where no excess Ar or Ar loss was identified (Fig. 4, 6). On the other hand, $^{40}Ar/^{39}Ar$ ages for Toomba and Kinrara are younger than the K-Ar ages, confirming the conclusions of both Griffin & McDougall (1975) and Wyatt & Webb (1971) that the K-Ar measurements for these flows were maximum ages.

5.2 Comparison with radiocarbon results

Radiocarbon analyses were undertaken on carbonized wood in sediments beneath the Toomba flow (Stephenson et al., 1978). Only a brief summary of the locality, samples, and analytical results were reported (Stephenson et al., 1978), and additional information is required to evaluate radiocarbon results (van der Plicht and Hogg, 2006). We have therefore found the full descriptions in the Australian National University archives and calculated calibrated radiocarbon ages (Fig. 7, Appendix B) using the most recent calibration for southern hemisphere terrestrial samples, SHCal 13 (Hogg et al., 2013).

The calibrated radiocarbon ages range from <2.5 to ~16 ka BP (Fig. 7). As noted by Stephenson et al. (1978), three of the results are young outliers (<7 ka BP), and when compared to the Toomba $^{40}Ar/^{39}Ar$ age (21 ± 3/3 ka, Fig. 7), can be excluded as being substantially contaminated by younger carbon. Although unfortunate, such contamination is not unexpected given the challenging sampling conditions, with: (1) modern rootlets present in the sediments (avoided as far as was possible); (2) moss covering exposed surfaces (also avoided); (3) the sampling site being inundated by the Burdekin River for approximately three months per year; and (4) the sediments remaining moist for the remainder of the year due to solar shielding by overhanging lava and the sediments acting as an aquifer. All of these factors increase the likelihood of contamination from carbon-bearing material younger than the Toomba lava.

Despite these challenges, the four older (>10 ka calibrated BP) radiocarbon analyses approach the $^{40}Ar/^{39}Ar$ eruption (and sediment burial) age for the flow (Fig. 7), a commendable outcome for bulk radiocarbon analyses of challenging samples. Additional radiocarbon analyses employing accelerator mass spectrometry and modern sample-preparation techniques may therefore have an excellent chance of obtaining the burial age for sediments beneath the Toomba and Kinrara flows – especially if sampling sites less susceptible to contamination could be found. New radiocarbon analyses would be beneficial because calibrated radiocarbon dates are more precise than $^{40}Ar/^{39}Ar$ analyses for these very young samples.

5.3: North Queensland volcanism in Aboriginal verbal tradition

The four $^{40}Ar/^{39}Ar$ ages conclusively show that voluminous mafic volcanism in north Queensland extended through the Pleistocene and well into the Holocene (Fig. 4, 5, 6). Aboriginal Australian peoples have lived on the continent for at least 50 ka (Thorne et al., 1999; Bowler et al., 2003), and could therefore have witnessed the youngest eruptions in north Queensland, especially Kinrara. The eruption of Kinrara was a major volcanic event, possibly spanning many years (Stephenson et al., 1998), and it produced lava flows that extend tens of kilometres down the Burdekin River valley (Fig. 2). As the Burdekin River is a prominent watercourse in a region that experiences long droughts and annual wet/dry seasons, it was therefore an area of higher human use than the surrounding countryside (Leichhardt, 1847), and volcanic events in this valley would presumably have been highly memorable.

The Gugu Badhun Aboriginal people inhabited the upper Burdekin River valley in the eastern part of the McBride volcanic province (Hoolihan and Sutton, 1970; James, 2009). One Gugu Badhun tradition recounts the earth being on fire along the watercourses, while a second tradition tells of a time when a witchdoctor made a pit in the ground and lots of dust in the air; people got lost in the dust, and died (Hoolihan and Sutton, 1970). We speculate that these features could be consistent with the geology of Kinrara, which erupted from a crater (Fig 3e), with ash-rich explosive activity, lava fountaining, and pyroclastic eruptions (Stanton, 1993). The mention of people dying in the dust (potentially volcanic ash) may be significant, as it could indicate noxious gas emissions during the eruption, or asphyxiation in the ash.

Although it is not possible to prove that these traditions were inspired by the Kinrara eruption, we consider that this volcanic event is a plausible explanation for descriptions of dust (potential volcanic ash) emanating from a pit in the ground, and for an event that caused the earth to burn – particularly along watercourses. Other natural phenomena are less likely as explanations for the traditions – there are no known impact craters in northeast Queensland (i.e., to explain a pit with dust), while severe bushfires or dust storms would not be restricted to a single pit or just the watercourses.

If these verbal traditions do recount eruption of Kinrara, it requires the traditions to have been passed down for 7 ± 2 ka (Table 1), spanning 230 ± 70 generations (at 30 years per generation, Tremblay and Vézina, 2000). This is a remarkably long period of time, equalling or exceeding the oldest written historical records in Mesopotamia and Egypt (~5 ka, Woods et al., 2010). Such longevity of verbal traditions has been hypothesised elsewhere in Australia, for events such as early Holocene sea level rise, volcanic activity in the late Pleistocene and Holocene, and potential meteorite falls (Smith, 1880; Hamacher and Norris, 2009; Murray-Wallace, 2011). We suggest that a worthwhile topic for future research would be to further examine Aboriginal verbal traditions for features that may describe eruptions, which may reveal information about these volcanoes, as well as the longevity and detail of the verbal traditions themselves.

5.4 Eruption frequency in northern Queensland

From a hazards point of view, understanding eruption frequency and patterns of volcanic activity through time is an important facet in examining past eruptions, and assessing the potential of what could happen in the future. We have therefore compiled a database of all chronologic analyses from north Queensland (Fig. 8, Appendix B). This database comprises 337 individual analyses on 235 eruptive units, and includes 179 previously unpublished K-Ar and radiocarbon results. This database is therefore a valuable resource to examine north Queensland volcanism through time (Appendix B). This chronologic dataset for north Queensland, including the new $^{40}Ar/^{39}Ar$ ages from this study, demonstrate that volcanic activity in north Queensland has been on-going since at least 9 Ma, with no significant temporal gaps (Fig. 8). There are no spatial trends in the volcanic distribution, with essentially random distribution of ages with respect to latitude or longitude (Fig. 8), confirming that this zone of intraplate volcanism is not plume derived. Significantly, the most volcanically active period is the last 2 Ma (Fig. 8), with 91 dated eruptions, which equates to an average of one eruption every 22 ka.

The actual eruption rate in northern Queensland is more frequent than indicated by this calculation, as there are many undated eruptions. In particular, many of the youngest volcanoes have not been analysed, as they were considered too young to yield accurate results by K-Ar (e.g., Whitehead et al., 2007). The lack of ages for young eruptions is exemplified by the Atherton province, which alone has at least 29 undated volcanoes that are likely <1 Ma, and in cases <<50 ka, based on their morphology (Whitehead et al., 2007). An additional issue is that numerous units were considered unsuitable for K-Ar analysis due to the rigorous – and necessary – screening protocol rejecting samples containing weathering phases, devitrified glass, or xenoliths (Wyatt and Webb, 1971; Griffin and McDougall, 1975; Coventry et al., 1985; Whitehead et al., 2007). Older units, which have been exposed at the surface for longer, can be particularly affected by weathering. Older units can also be buried, or the flow boundaries obscured by weathering. The net result is that the existing chronology in northern Queensland is somewhat biased towards flows of intermediate age, with the youngest flows being under-represented as they have historically been the most challenging to analyse, while the oldest eruptions are under-represented due to their increased weathering, burial, and/or difficulty to map and sample as distinct units.

A further complication with the current chronology is the dominance of K-Ar analyses, which comprise >92% of the dataset (Appendix B). Although in ideal circumstances a K-Ar analysis will yield the same age as $^{40}Ar/^{39}Ar$ (albeit with the K-Ar analysis generally yielding poorer precision, e.g., Undara), if rocks contain excess Ar or have experienced Ar loss, the K-Ar system can yield results that are too old or too young, respectively (McDougall and Harrison, 1999). Therefore, despite the considerable number of age analyses in north Queensland (Fig. 8, Appendix B), there are likely still details of the volcanic history that may be obscured by gaps in the database and the lower precision and/or accuracy of the K-Ar system.

As an alternate, albeit approximate, estimate of eruption frequency, we have divided the number of mapped eruption points by the duration of activity. There are at least 306 recognised volcanic events within the McBride, Nulla, Sturgeon, and Chudleigh provinces (Stephenson et al., 1998), 54 in Atherton (Whitehead et al., 2007), 18 in McLean, 14 in Piebald, 4 in Wallaroo, and one at Mount Fox (Stephenson, 1989). There are therefore at least 397 eruption events in north Queensland – although this is still a minimum estimate given the potential for older structures to be buried or otherwise not mapped. These 397 recognized eruptions are largely from extant cinder cones and craters with prominent topographic exposure, and are dominantly less than ~4 Ma (Stephenson, 1989), which equates to an average of one eruption every 10 ka. For comparison, this is only moderately less frequent than the eruption rate in the better-known Auckland volcanic field, which over the last 140 ka has on average ~3 ka between eruptions (Smith and Allen, 1993), with as little as ~1.8 ka between eruptions around 30 ka ago (Bebbington and Cronin, 2010).

We conclude that the average recurrence interval for volcanism in northern Queensland is less than 10-22 ka between eruptions, using two different calculation methods. We note that the actual eruption rate is likely more frequent than either of these estimates, as the numbers of eruptions dated and mapped are minimum values. Also, by analogy with other intraplate volcanoes (e.g., Auckland, Bebbington and Cronin, 2010), the eruption frequency likely fluctuated through time. Nevertheless, the relatively short average recurrence interval, when combined with the youthfulness of the most recent eruptions like Kinrara (Table 1) and additional probable Holocene eruptions in the Atherton province (Whitehead et al., 2007), indicates that volcanism in northern Queensland has the potential for future activity.

Ideally we would also investigate the lava flux through time, but such volumetric information for individual eruptions is not available for most north Queensland volcanoes. Where data is available in the Atherton province, increased magma output was observed from 3.5 to 3 Ma and 2 to 1 Ma (Whitehead et al., 2007). Nevertheless, the presence of very long late Pleistocene and Holocene lava flows in the McBride, Nulla, Sturgeon, and Chudleigh provinces indicate these areas experienced significant magma production in the recent past.

Given the known spatial-temporal gaps and analytical challenges in the existing chronological and volumetric dataset, a comprehensive future campaign is required to fully establish the Quaternary eruption history in northern Queensland. The results of this study, and similar studies (e.g., Matchan and Phillips, 2014) indicate that multi-collector $^{40}Ar/^{39}Ar$ incremental-heating of acid-treated samples is able to provide ages for young mafic volcanic events. If increased precision is required for the youngest eruptions, radiocarbon, thermoluminescence, or optically stimulated luminescence analyses may also be beneficial (e.g., Sherwood et al., 2004; Gillen et al., 2010). We recommend that such an integrated chronological study, combined with detailed mapping of the region to find new flows/eruptions and an examination of erupted volumes through time, is required to evaluate the volcanic history and future hazard in north Queensland, Australia. Such a study would provide information on the frequency and eruption patterns at this long-lived region of intraplate volcanic activity.

6. Conclusions

Despite the Australian continent not being exactly synonymous with young volcanism, multi-collector $^{40}Ar/^{39}Ar$ chronology from four long lava flows in northern Queensland has conclusively confirmed that eruptions extend from the latest Pleistocene well into the Holocene. Ages obtained are 189 ± 4/4 ka at Undara, 153 ± 5/5 at Murronga, 21 ± 3/3 ka at Toomba, and 7 ± 2/2 ka at Kinrara (2σ, full analytical/external uncertainty). The Holocene eruption of Kinrara may feature in the verbal traditions of the Gugu Badhun people, which would indicate that these verbal traditions have been passed down for 230 ± 70 generations (at 30 years per generation). Our compilation of 337 age analyses on 235 volcanic events in north Queensland indicates an average frequency of <10-22 ka between eruptions. Since eruptions in the region have been on going since at least 9 Ma, volcanism in northern Queensland should be considered potentially active. There are, however, known gaps and analytical issues in the existing age dataset, so to fully and reliably evaluate the eruption frequency and volcanic hazard requires further chronologic investigation of this region.

Acknowledgements

This study benefited considerably from the extensive suite of 168 previously unpublished K-Ar ages provided by the late P.J. Stephenson. Jon passed away in 2011, and although he did not have the opportunity to be involved in the $^{40}Ar/^{39}Ar$ work, we think he would be excited about the results, and keen to see further studies on this widespread region of young volcanism. The authors of this study acknowledge Ian McDougall and Shane Paxton for assistance in supplying rock samples; Ross Dymock, Dan Barfod, and Jim Imlach for $^{40}Ar/^{39}Ar$ analytical assistance; Google Earth, Zoe Martin, Warwick Willmott, and Stephen Mattox for field images; and the Australian Institute of Aboriginal and Torres Strait Islander Studies for information about Gugu Badhun verbal traditions. Ian McDougall and Godfrey Fitton provided valuable feedback and discussions, and we are grateful for their input. $^{40}Ar/^{39}Ar$ analytical costs were supported by the SUERC Argon Isotope Facility. We appreciate the detailed manuscript reviews by D. Phillips and an anonymous reviewer, and thank S. Nomade for the editorial handling of the paper.

Appendix A. Supplementary $^{40}Ar/^{39}Ar$ data.

Appendix B. Compilation of chronologic analyses from north Queensland.

Supplementary data related to this article can be found at *INSERT WEBLINK*. There are two supplementary datasets comprising: Appendix A, an Excel table with full $^{40}Ar/^{39}Ar$ analytical results; and Appendix B, an Excel table with a compilation of ages for north Queensland volcanoes.

References

Alexander, J., Fielding, C.R., Wakefield, S.J., George, M.T., Cottnam, C.F., 2001. Fluvial Geochemistry through a Short-Duration, Tropical-Cyclone Induced

Discharge event in the Burdekin River and Hann Creek, North Queensland, Australia. Aquatic Geochemistry 7, 275-293.
Atkinson, A., Griffin, T.J., Stephenson, P.J., 1975. A Major Lava Tube System from Undara Volcano, North Queensland. Bulletin Volcanologique 39, 266-293.
Atkinson, A., Atkinson, V., 1995. Undara Volcano and its Lava Tubes. Vernon & Anne Atkinson, Brisbane.
Atkinson, A., 2010. Undara Volcano, North Queensland, Australia and its Lava Field – Lava Caves, Depressions and The Wall – a Possible Lunar Analogue. Proceedings 14th International Symposium on Vulcanospeleology, pp. 19-44.
Bebbington, M.S., Cronin, S.J., 2010. Spatio-temporal hazard estimation in the Auckland Volcanic Field, New Zealand, with a new event-order model. Bulletin of Volcanology 73, 55-72. doi:10.1007/s00445-010-0403-6
Bowler, J.M., Johnston, H., Olley, J.M., Prescott, J.R., Roberts, R.G., Shawcross, W., Spooner, N.A., 2003. New ages for human occupation and climatic change at Lake Mungo, Australia. Nature 421, 837-840. doi:10.1038/nature01383
Boyce, J., 2013. The Newer Volcanics Province of southeastern Australia: a new classification scheme and distribution map for eruption centres. Australian Journal of Earth Sciences 60, 449-462. doi:10.1080/08120099.2013.806954
Bronk Ramsey, C., 1995. Radiocarbon Calibration and Analysis of Stratigraphy: The OxCal Program. Radiocarbon 37, 425-430.
Bronk Ramsey, C., 2001. Development of the Radiocarbon Program OxCal. Radiocarbon 43, 355-363.
Burch, A.T., 1991. Flow discrimination in the Toomba Basalt, BSc. (Honours) thesis, James Cook University of North Queensland.
Cohen, B.E., Knesel, K.M., Vasconcelos, P.M., Thiede, D.S., Hergt, J.M., 2008. $^{40}Ar/^{39}Ar$ constraints on the timing and origin of Miocene leucitite volcanism in southeastern Australia. Australian Journal of Earth Sciences 55, 407-418. doi:10.1080/08120090701769514
Cohen, B.E., Knesel, K.M., Vasconcelos, P.M., Schellart, W.P., 2013a. Tracking the Australian plate motion through the Cenozoic: Constraints from $^{40}Ar/^{39}Ar$ geochronology. Tectonics 32, 1371-1383. doi:10.1002/tect.20084
Cohen, B.E., Withnall, I.M., Vasconcelos, P.M., 2013b. Intraplate magmatism of eastern Queensland. In: Jell, P.A. (Ed.), The Geology of Queensland. Geological Survey of Queensland, Brisbane, pp. 629-645.
Conrad, C.P., Bianco, T.A., Smith, E.I., Wessel, P., 2011. Patterns of intraplate volcanism controlled by asthenospheric shear. Nature Geoscience 4, 317-321. doi:10.1038/NGEO1111
Coventry, R.J., Stephenson, P.J., Webb, A.W., 1985. Chronology of landscape evolution and soil development in the upper Flinders River area, Queensland, based on isotope dating of Cainozoic basalts. Australian Journal of Earth Sciences 32, 433-447.
Davies, D.R., Rawlinson, N., 2014. On the origin of recent intraplate volcanism in Australia. Geology 42, 1031-1034. doi:10.1130/g36093.1
Davies, D.R., Rawlinson, N., Iaffaldano, G., Campbell, I.H., 2015. Lithospheric controls on magma composition along Earth's longest continental hotspot track. Nature 525, 511-514. doi:10.1038/nature14903
Demidjuk, Z., Turner, S., Sandiford, M., George, R., Foden, J., Etheridge, M., 2007. U-series isotope and geodynmaic constraints on mantle melting processes beneath the Newer Volcanic Province in South Australia. Earth and Planetary Science Letters 261, 517-533.

Espanon, V.R., Chivas, A.R., Phillips, D., Matchan, E.L., Dosseto, A., 2014. Geochronological, morphometric and geochemical constraints on the Pampas Onduladas long basaltic flow (Payún Matrú Volcanic Field, Mendoza, Argentina). Journal of Volcanology and Geothermal Research 289, 114-129. doi:10.1016/j.jvolgeores.2014.10.018

Fielding, C.R., Alexander, J., 1996. Sedimentology of the Upper Burdekin River of North Queensland, Australia - an example of a tropical, variable discharge river. Terra Nova 8, 447-457.

Fleck, R.J., Sutter, J.F., Elliot, D.H., 1977. Interpretation of discordant $^{40}Ar/^{39}Ar$ age-spectra of Mesozoic tholeiites from Antarctica. Geochimica et Cosmochimica Acta 41, 15-32.

Gillen, D., Honda, M., Chivas, A.R., Yatsevich, I., Patterson, D.B., Carr, P.F., 2010. Cosmogenic ^{21}Ne exposure dating of young basaltic lava flows from the Newer Volcanic Province, western Victoria, Australia. Quaternary Geochronology 5, 1-9. doi:10.1016/j.quageo.2009.08.004

Griffin, T.J., McDougall, I., 1975. Geochronology of the Cainozoic McBride volcanic province, northern Queensland. Journal of the Geological Society of Australia 22, 387-396.

Griffin, T.J., 1977. The Geology Mineralogy and Geochemistry of the McBride Basaltic Province, Northern Queensland, PhD thesis, James Cook University of North Queensland.

Hamacher, D.W., Norris, R.P., 2009. Australian Aboriginal Geomythology: Eyewitness Accounts of Cosmic Impacts? Archaeoastronomy 22, 60-93.

Hogg, A.G., Hua, Q., Blackwell, P.G., Niu, M., Buck, C.E., Guilderson, T.P., Heaton, T.J., Palmer, J.G., Reimer, P.J., Reimer, R.W., Turney, C.S.M., Zimmerman, S.R.H., 2013. SHCal 13 Southern Hemisphere Calibration, 0-50,000 Years Cal BP. Radiocarbon 55, 1889-1903. doi:10.2458/azu_js_rc.55.16783

Hoolihan, D., Sutton, P., 1970. AIATSIS Library Reference MS379 P91, Field Tape 70/2 (Sutton_P08_001800B) & Tape 70/10 (Sutton_P08_001804B).

James, R.A., 2009. A Modern History of the Gugu Badhun People and their Country, Master of Indigenous Studies (Hons) thesis, James Cook University.

Johnson, R.W., 1989. Intraplate Volcanism in Eastern Australia and New Zealand. Cambridge University Press, Cambridge.

Keszthelyi, L., Self, S., 1998. Some physical requirements for the emplacement of long basaltic lava flows. Journal of Geophysical Research 103, 27,447-427,464.

Knesel, K.M., Cohen, B.E., Vasconcelos, P.M., Thiede, D.S., 2008. Rapid change in drift of the Australian plate records collision with Ontong Java plateau. Nature 454, 754-757. doi:10.1038/nature07138

Lee, J.-Y., Marti, K., Severinghaus, J.P., Kawamura, K., Yoo, H.-S., Lee, J.B., Kim, J.S., 2006. A redetermination of the isotopic abundances of atmospheric Ar. Geochimica et Cosmochimica Acta 70, 4507-4512. doi:10.1016/j.gca.2006.06.1563

Leichhardt, L., 1847. Journal of an overland expedition in Australia, from Moreton Bay to Port Essington, a distance of upwards of 3000 miles, during the years 1844-1845. T. and W. Boone, London.

Lister, G.S., Etheridge, M.A., 1989. Detachment Models for Uplift and Volcanism in the Eastern Highlands, and their Application to the Origin of Passive Margin Mountains. In: Johnson, R.W. (Ed.), Intraplate Volcanism in Eastern Australia and New Zealand. Cambridge University Press, Cambridge, pp. 297-313.

Mark, D.F., Barfod, D., Stuart, F.M., Imlach, J., 2009. The ARGUS multicollector noble gas mass spectrometer: Performance for $^{40}Ar/^{39}Ar$ geochronology. Geochemistry, Geophysics, Geosystems 10, Q0AA02. doi:10.1029/2009GC002643

Mark, D.F., Stuart, F.M., de Podesta, M., 2011. New high-precision measurements of the isotopic composition of atmospheric argon. Geochimica et Cosmochimica Acta 75, 7494-7501. doi:10.1016/j.gca.2011.09.042

Matchan, E.L., Phillips, D., 2014. High precision multi-collector $^{40}Ar/^{39}Ar$ dating of young basalts: Mount Rouse volcano (SE Australia) revisited. Quaternary Geochronology 22, 57-64. doi:10.1016/j.quageo.2014.02.005

McDougall, I., Harrison, T.M., 1999. Geochronology and Thermochronology by the $^{40}Ar/^{39}Ar$ Method, 2nd ed. Oxford University Press, New York.

Murray-Wallace, C.V., 2011. Comment on: “New $^{40}Ar/^{39}Ar$ ages for selected young (<1 Ma) basalt flows of the Newer Volcanic Province, southeastern Australia” by E. Matchan & D. Phillips. Quaternary Geochronology 6, 598-599. doi:10.1016/j.quageo.2011.07.001

Niespolo, E.M., Rutte, D., Deino, A.L., Renne, P.R., in press. Intercalibration and age of the Alder Creek sanidine $^{40}Ar/^{39}Ar$ standard. Quaternary Geochronology. doi:dx.doi.org/10.1016/j.quageo.2016.09.004

Renne, P.R., Balco, G., Ludwig, K.R., Mundil, R., Min, K., 2011. Response to the comment by W.H. Schwarz et al. on "Joint determination of ^{40}K decay constants and $^{40}Ar^{*}/^{40}K$ for the Fish Canyon sanidine standard, and improved accuracy for $^{40}Ar/^{39}Ar$ geochronology" by Paul R. Renne et al. (2010). Geochimica et Cosmochimica Acta 75, 5097-5100. doi:10.1016/j.gca.2011.06.021

Renne, P.R., Deino, A.L., Hilgen, F.J., Kuiper, K.F., Mark, D.F., Mitchell, W.S.I., Morgan, L.E., Mundil, R., Smit, J., 2013. Time Scales of Critical Events Around the Cretaceous-Paleogene Boundary. Science 339, 684-687. doi:10.1126/science.1230492

Self, S., Keszthelyi, L., Thordanson, T., 1998. The Importance of Pahoehoe. Annual Review of Earth and Planetary Sciences 26, 81-110.

Sherwood, J., Oyston, B., Kershaw, A.P., 2004. The age and contemporary environments of Tower Hill volcano, southwest Victoria, Australia. Proceedings of the Royal Society of Victoria 116, 71-78.

Smith, C., 1880. Booandik Tribe of South Australian Aborigines: A Sketch of their Habits, Customs, Legends and Language. Government Printer, Adelaide.

Smith, I.E.M., Allen, S.R., 1993. Volcanic hazards at the Auckland volcanic field. Ministry of Civil Defence. Volcanic hazards information series 5, Wellington.

Stanton, D., 1993. Morphology and geochemistry of the Kinrara volcano and lava field: An examination of a Holocene volcanic feature in the McBride lava province, North Queensland., BSc. (Honours) thesis, James Cook University.

Stephenson, P.J., Griffin, T.J., 1976. Some long basaltic flows in north Queensland. In: Johnson, R.W. (Ed.), Volcanism in Australasia: a collection of papers in honour of the late G.A.M. Taylor. Elsevier, Amsterdam, pp. 41-51.

Stephenson, P.J., Polach, H.A., Wyatt, D.H., 1978. The age of the Toomba basalt, north Queensland. in: Stephenson, P.J. (Ed.). Third Australian Geological Convention. Geological Society of Australia, Townsville, pp. 62-63.

Stephenson, P.J., 1989. Northern Queensland. In: Johnson, R.W. (Ed.), Intraplate volcanism in eastern Australia and New Zealand. Cambridge University Press, Cambridge, pp. 89-97.

Stephenson, P.J., Burch-Johnson, A.T., Stanton, D., Whitehead, P.W., 1998. Three long lava flows in north Queensland. Journal of Geophysical Research 103, 27359-27370.

Sutherland, F.L., Graham, I.T., Meffre, S., Zwingmann, H., Pogson, R.E., 2012. Passive-margin prolonged volcanism, East Australian Plate: outbursts, progressions, plate controls and suggested causes. Australian Journal of Earth Sciences 59, 983-1005. doi:dx.doi.org/10.1080/08120099.2012.688293

Thorne, A., Grün, R., Mortimer, G., Spooner, N.A., Simpson, J.J., McCulloch, M.T., Taylor, L., Curnoe, D., 1999. Australia's oldest human remains: Age of the Lake Mungo 3 skeleton. Journal of Human Evolution 36, 591-612.

Tremblay, M., Vézina, H., 2000. New estimates of intergenerational time intervals for the calculation of Age and Origins of Mutations. American Journal of Human Genetics 66, 651-658.

van der Plicht, J., Hogg, A., 2006. A note on reporting radiocarbon. Quaternary Geochronology 1, 237-240. doi:10.1016/j.quageo.2006.07.001

Vasconcelos, P.M., Knesel, K.M., Cohen, B.E., Heim, J.A., 2008. Geochronology of the Australian Cenozoic: a history of tectonic and igneous activity, weathering, erosion, and sedimentation. Australian Journal of Earth Sciences 55, 865-914. doi:10.1080/08120090802120120

Wellman, P., McDougall, I., 1974. Cainozoic igneous activity in eastern Australia. Tectonophysics 23, 49-65.

Whitehead, P.W., Stephenson, P.J., 1998. Lava rise ridges of the Toomba basalt flow, north Queensland, Australia. Journal of Geophysical Research 103, 27371-27382.

Whitehead, P.W., Stephenson, P.J., McDougall, I., Hopkins, M.S., Graham, A.W., Collerson, K.D., Johnson, D.P., 2007. Temporal development of the Atherton Basalt Province, north Queensland. Australian Journal of Earth Sciences 54, 691-709. doi:10.1080/08120090701305236

Wijbrans, J., Schneider, B., Kuiper, K., Calvari, S., Branca, S., De Beni, E., Norini, G., Corsaro, R.A., Miraglia, L., 2011. $^{40}Ar/^{39}Ar$ geochronology of Holocene basalts; examples from Stromboli, Italy. Quaternary Geochronology 6, 223-232. doi:10.1016/j.quageo.2010.10.003

Wilson, J.T., 1963. A possible origin of the Hawaiian Islands. Canadian Journal of Physics 41, 863-870.

Woods, C., Emberling, G., Teeter, E., 2010. Visible Language: Invention of Writing in the Ancient Middle East And Beyond. The University of Chicago.

Wyatt, D.H., Webb, A.W., 1971. Potassium-argon ages of some northern Queensland basalts and an interpretation of Late Cainozoic history. Journal of the Geological Society of Australia 17, 39-51.

Fig. 1. Quaternary and late Neogene volcanism in northern Queensland forms part of the extensive Cenozoic activity spanning most of the east Australian margin (Wellman and McDougall, 1974; Cohen et al., 2013a). Lava-field provinces are shaded grey, central volcanoes are shaded black. Areas mentioned in the text are labelled.

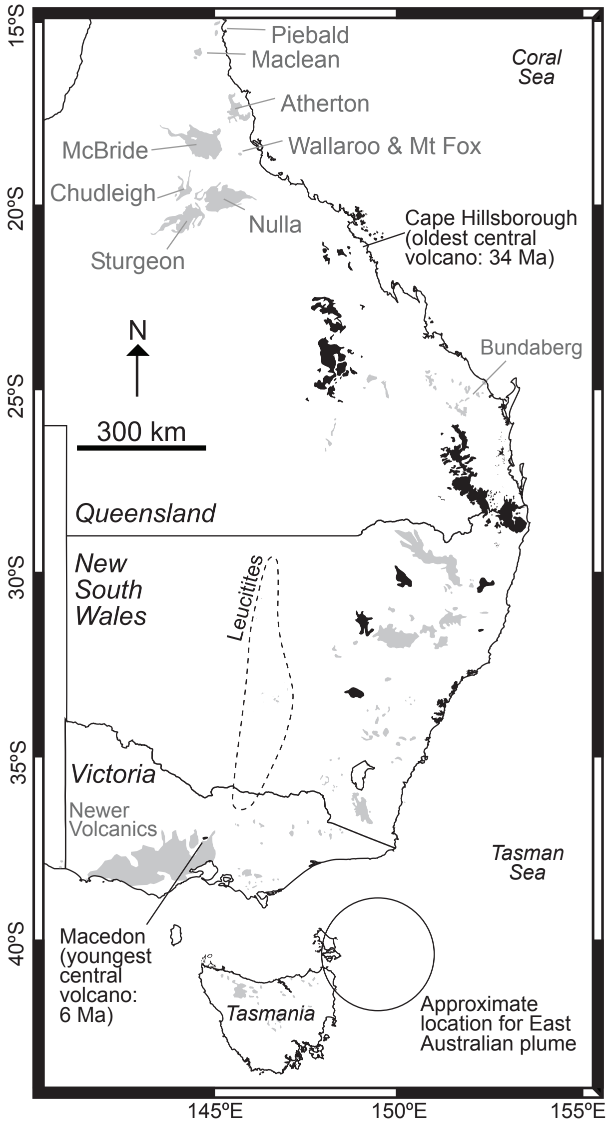

Fig. 2. Digital elevation model of North Queensland, showing the morphology of the long lava flows, and the abundance of young volcanic cones in the McBride, Chudleigh, Sturgeon, and Nulla provinces, with over 306 eruption points recognized (Stephenson et al., 1998). The Undara flow is outlined in purple, Murronga in black, Kinrara in orange, and Toomba in red, while all other volcanic units are outlined in grey. Yellow diamonds indicate sampling sites. Unit boundaries are from the Geological Survey of Queensland, and elevation data is from NASA SRTM.

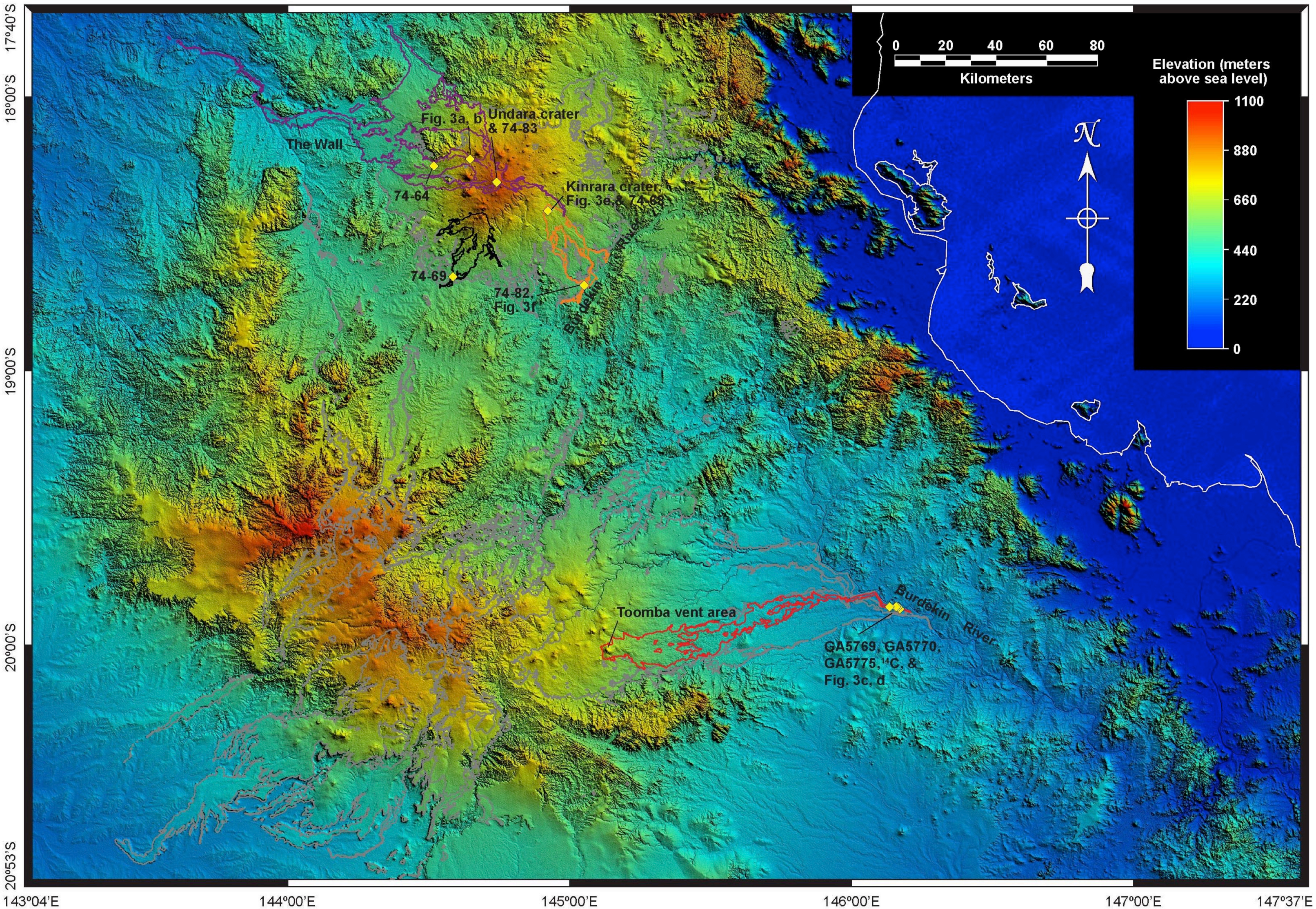

0 20 40 60 80
Kilometers
Elevation (meters above sea level)
1100
880
660
440
220
0
N
The Wall
Fig. 3a, b
Undara crater & 74-83
74-64
Kinrara crater, Fig. 3e, & 74-68
74-69
74-82, Fig. 3f
Burdekin River
Toomba vent area
Burdekin River
GA5769, GA5770, GA5775, ¹⁴C, & Fig. 3c, d
17°40'S
18°00'S
19°00'S
20°00'S
20°53'S
143°04'E
144°00'E
145°00'E
146°00'E
147°00'E
147°37'E

Fig. 3. Field images of north Queensland volcanism. (a) Aerial view of part of the Undara lava system, with a series of wide collapse depressions that host dark vegetation due to a greater water supply compared to the surrounding plains. At this location the Undara lavas (which flowed from right to left) passed the older Kalkani scoria cone, ~800 m wide, located at the top of the image. Image from Google Earth Pro 2016 Cnes/Astrium. (b) The entrance to the Wind Tunnel lava tube, ~8 m high, with horizontal lines on the tube walls representing former lava levels (best visible on the walls near the cave entrance). The white and orange areas are minerals precipitated by groundwater. Walkway is ~0.5 m wide, photo by Z. Martin, 2015. (c) The exposed pāhoehoe lava surface of the Toomba flow at Lowes Basin, which remains fresh with surface features preserved despite the location in the tropics. Note that the fragments on the flow surface in the upper part of the image are broken pieces of pāhoehoe. Vegetation is only present in areas not covered by lava, or in cracks through the lava. (d) Close view of the fresh pāhoehoe surface of the Toomba flow at Lowes Basin, camera case ~10 cm long for scale. Photos (c) and (d) by W. Willmott, 2008. (e) Kinrara crater, 300-400 meters wide and 86 meters deep, dark collapsed lava tubes and lava channels to the northeast and south of the crater, aerial view from Google Earth Pro 2016 Cnes/Spot. (f) Fresh pāhoehoe lava surface of the Kinrara lava flow near the Burdekin River road crossing, people for scale, photo by S. Mattox, 1996.


(a)
(b)
(c)
(d)
(e)
(f)

Fig. 4. $^{40}Ar/^{39}Ar$ incremental-heating results from Undara and Murronga. The spectra have plateaus comprising 100% of the ^{39}Ar released. Both samples from Undara also yield concordant ages. Uncertainties are two-sigma, and include the uncertainty in J and decay constants.

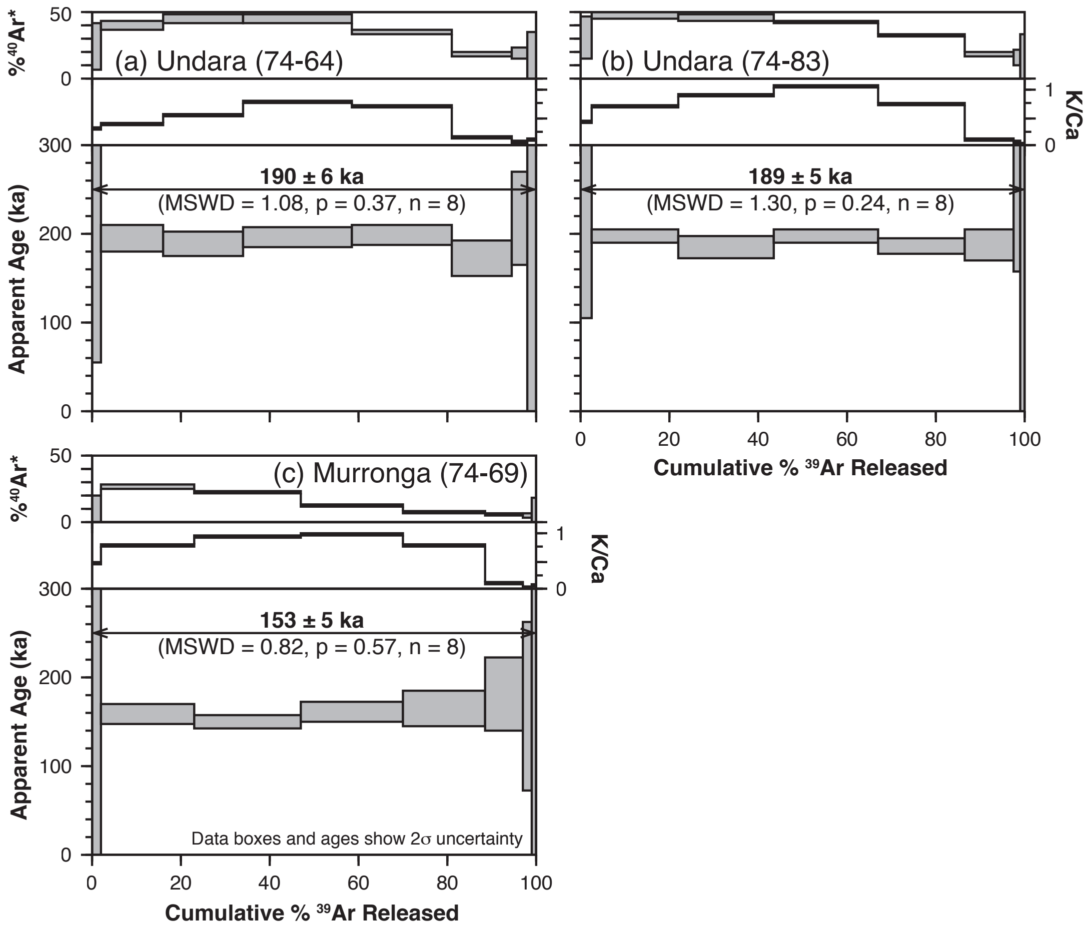

Fig. 5. $^{40}Ar/^{39}Ar$ incremental-heating results from Toomba and Kinrara. The spectra have plateaus comprising from 98 to 100% of the ^{39}Ar released, and all analyses from Toomba and Kinrara, respectively, yield concordant plateau ages. Uncertainties are two-sigma, and include the uncertainty in J and decay constants.

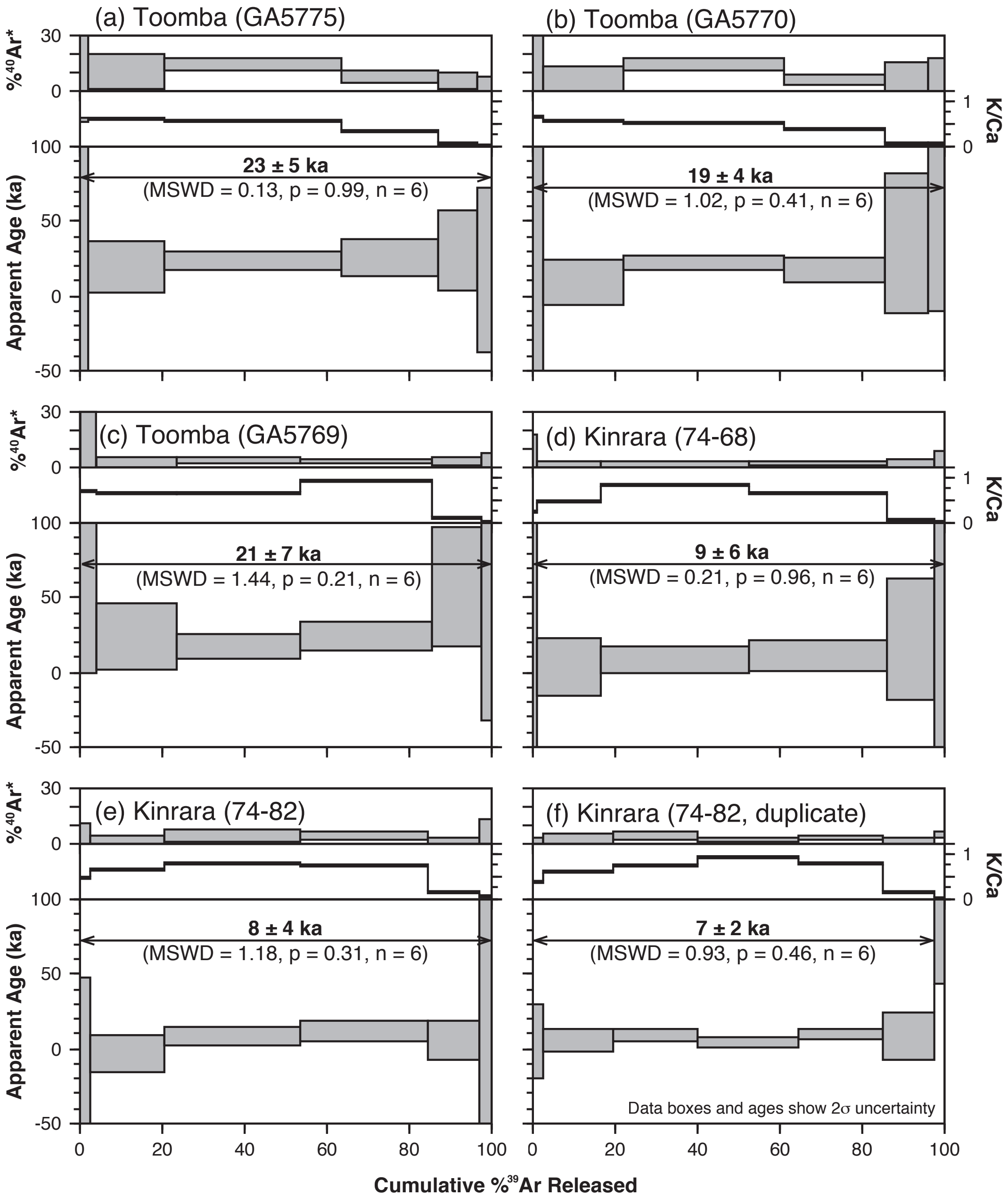

Fig. 6. Inverse isochron analysis for all samples. Results from each of the four flows yield single linear age populations, MSWD <2, and initial $^{40}Ar/^{36}Ar$ intercepts within uncertainty of modern-day atmosphere. The magenta ellipse (indicated by a magenta arrow) is an outlier eliminated from the inverse isochron analysis of Kinrara, and the orange dashed lines indicate two-sigma uncertainty envelope. "Atm." indicates modern-day atmosphere (Lee et al., 2006). Uncertainties are two-sigma, and include the uncertainty in J and decay constants.

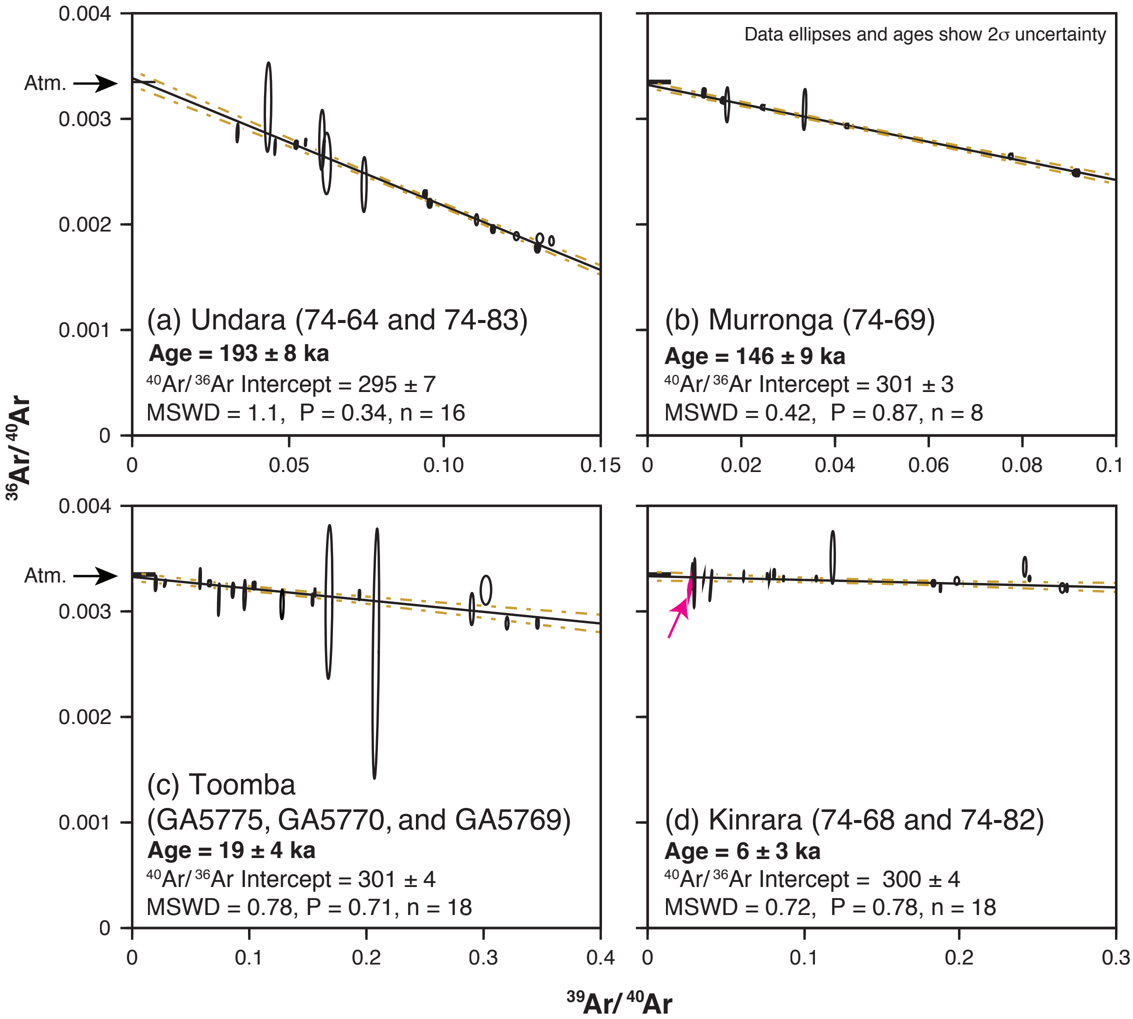

Fig. 7. Calibrated radiocarbon ages from sediments beneath the Toomba flow at the banks of the Burdekin River. Dates with two-sigma uncertainty bars were calculated using OxCal v4.2.4 (Bronk Ramsey, 1995, 2001) and the southern hemisphere terrestrial calibration curve (Hogg et al., 2013). The radiocarbon dates are younger than the $^{40}Ar/^{39}Ar$ age for Toomba, indicating the ^{14}C samples experienced variable contamination by younger carbon.

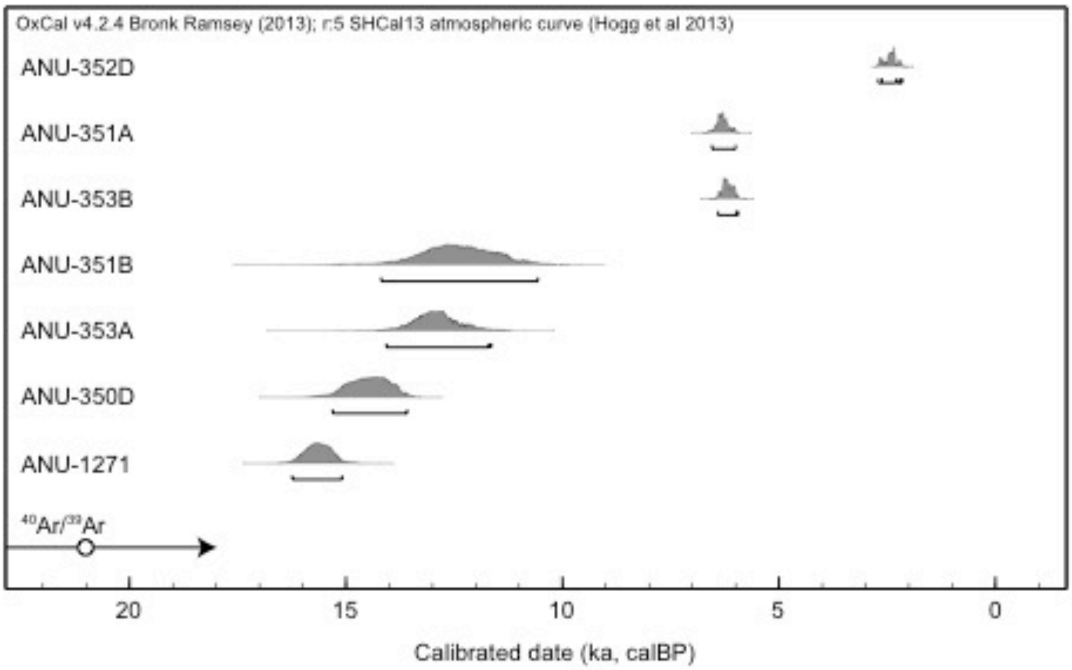

Fig. 8. Summary of ages for north Queensland, data from Appendix B. (a) Volcanism in north Queensland has been steadily ongoing since at least 9 Ma, with no significant breaks in activity. The most frequent activity occurred within the last 2 Ma (dashed line in (a), all of (b)), with 91 dated eruptions in this time period. (c) North Queensland ages versus latitude and (d) north Queensland ages versus longitude indicate that there are no evident time-space trends in activity, indicating that intraplate volcanism in this region is not due to a plume.

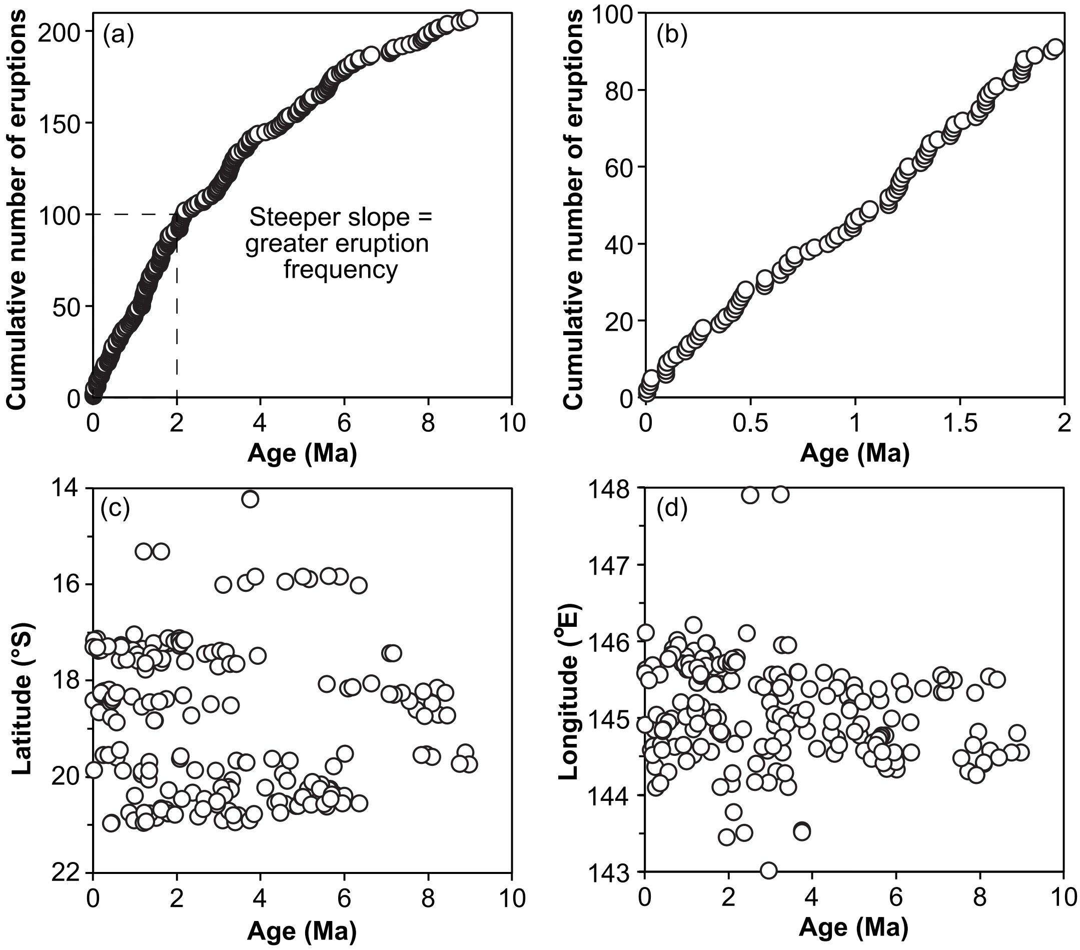

Table 1: Summary of $^{40}Ar/^{39}Ar$ and K-Ar ages and sample localities.

Volcano	$^{40}Ar/^{39}Ar$ weighted mean (ka ± 2σ)	$^{40}Ar/^{39}Ar$ isochron (ka ± 2σ)	$^{40}Ar/^{39}Ar$ plateau (ka ± 2σ)	Sample Number	K-Ar wt% K [1]	K-Ar %$^{40}Ar^{*}$ [1]	K-Ar age (ka ± 2σ)[1,2]	AMG66 Easting (m)[1,3]	AMG66 Northing (m)[1,3]	Longitude (°E) [1,3]	Latitude (°S) [1,3]	Location description
Undara	**189 ± 4/4**	193 ± 8/8	190 ± 6/6	74-64	1.349, 1.342	6.4	190 [180] ± 20	237400	7980100	144.51651	18.25239	27 km west of Undara Crater.
			189 ± 5/5	74-83	1.527, 1.526	16.9	200 [190] ± 10	261100	7973800	144.73977	18.31207	Northwest rim of Undara Crater.
Murronga	**153 ± 5/5**	146 ± 9/9	153 ± 5/5	74-69	1.736, 1.743	1.9	120 [120] ± 40	245200	7935400	144.58458	18.65698	Rosella Plains road.
						3.2	190 [180] ± 30					
Toomba	**21 ± 3/3**	19 ± 4/4	23 ± 5/5	GA5775	1.647, 1.643	4.3	56 [54] ± NA	410290	7804050	146.14323	19.85749	Burdekin River, at Big Bend.
			19 ± 4/4	GA5770	1.651, 1.647	3.9	82 [79] ± NA	409680	7804240	146.13740	19.85576	Burdekin River, at The Overflow.
			21 ± 7/7	GA5769	1.680, 1.686	1.8	46 [44] ± NA	407230	7804090	146.11396	19.85700	Near Burdekin River.
Kinrara	**7 ± 2/2**	6 ± 3/3	9 ± 6/6	74-68	1.768,1.751	5.2	53 [51] ± 7	279700	7962500	144.91443	18.41613	Lava tube, 300 m north of crater.
			8 ± 4/4	74-82	1.611, 1.615	9.3	74 [71] ± 5	294300	7932500	145.04951	18.68859	Burdekin River, ~40 km from crater.
			7 ± 2/2	74-82 duplicate				294300	7932500	145.04951	18.68859	Burdekin River, ~40 km from crater.

[1] Samples, locations, and K-Ar ages for Undara, Murronga, and Kinrara are from Griffin and McDougall (1975); grid references were reported as AMG66 easting and northing, and have a horizontal accuracy of ca. ± 100 m. Samples, locations, and K-Ar ages for Toomba are from Wyatt and Webb (1971); grid references were reported in 4-mile military grid co-ordinates and these were converted to AMG66 easting and northing by comparing the corresponding 4-mile and AMG66 topographic maps, and locations have an estimated horizontal accuracy of ± 300 m.

[2] K-Ar ages are recalculated to decay constants of Renne et al. (2011); the values in [square brackets] are those originally reported.

[3] Zone 55, Australian Map Grid 66.